

Rapid Communications

Segmentation of Large Brain Lesions

S. A. Hojjatoleslami and F. Kruggel*

Abstract—This paper describes a region-growing algorithm for the segmentation of large lesions in T_1 -weighted magnetic resonance (MR) images of the head. The algorithm involves a gray level similarity criterion to expand the region and a size criterion to prevent from over-growing outside the lesion. The performance of the algorithm is evaluated and validated on a series of pathologic three-dimensional MR images of the head.

Index Terms—Brain lesions, magnetic resonance imaging, segmentation.

I. INTRODUCTION

High-resolution T_1 -weighted magnetic resonance (MR) images of the brain are used in clinical practice to reveal focal lesions of the brain as consequences of head trauma, intracerebral hemorrhages, or cerebral infarcts. Properties of the lesion (i.e., position, extent, density) are known to be related to cognitive handicaps of a patient. While a *semi-quantitative* analysis of MR tomograms based on visual inspection (i.e., rating scales) is common today in certain clinical protocols, tools for a *quantitative* analysis are still rare. One of the reasons for this deficiency is that building reliable tools to segment MR images with pathological findings is considered a nontrivial task.

In this paper, we focus on the segmentation of focal brain lesions in their chronic stage. Such lesions are not necessarily complete, i.e., MR intensities of the lesion are found in the range between values of undamaged tissue and values similar to the cerebrospinal fluid (CSF), indicating a completely damaged area. Properties of a lesion are generally not homogeneous, often with completely damaged core parts and minor damage in peripheral portions. In addition, the boundary between a cortical lesion and the CSF compartment is often hard to draw.

Manual segmentation of such lesions is considered as the "gold standard." A human expert with anatomical knowledge, experience, and patience is required who uses some graphical software tool to outline the region of interest (ROI). While this method obviously produces the most reliable results, it is time consuming and tedious. Retests and interrater reliability studies of manually segmented lesion rarely reach 90% correspondence [1], [4], [11]. Previous studies in automatic lesion segmentation concentrated on white matter lesions occurring in multiple sclerosis (MS). Techniques suggested for this problem include: statistical clustering [10], a combination of statistical techniques and anatomical knowledge [5], an analysis of follow-up examinations [9], a combined classification of multichannel MR images [2], [12], or an iterative approach to correct B_1 field inhomogeneities while classifying voxels [8]. However, the problem studied in this paper is more general. Typically, MS lesions are covered by white matter, while focal lesions as consequences of head trauma or cerebral infarction generally include the cortical gray matter and, thus, reach the CSF compartment.

Manuscript received November 9, 1999; revised April 20, 2001. The Associate Editor responsible for coordinating the review of this paper and recommending its publication was M. Viergever. Asterisk indicates corresponding author.

S. A. Hojjatoleslami is with the Max-Planck-Institute of Cognitive Neuroscience, 04103 Leipzig, Germany.

*F. Kruggel is with the Max-Planck-Institute of Cognitive Neuroscience, Stephanstrasse 1, 04103 Leipzig, Germany (e-mail: kruggel@cns.mpg.de).

Publisher Item Identifier S 0278-0062(01)05364-2.

So the problem is to discriminate a lesion from *multiple* surrounding compartments.

Section II describes the segmentation procedure proposed here, which is basically a region-growing algorithm [3] governed by a new criteria, preventing the process from over-growing into adjacent low-intensity regions. The behavior of this algorithm is studied for segmenting lesions in data sets of patients with traumatic brain injuries. As an informal validation of the procedure, a comparison with manual segmentations in two cases is included. Finally, we discuss strengths, weaknesses, and extensions of this approach.

II. REGION GROWING

The region-growing method by pixel aggregation [3] is adopted for segmentation purposes with some modifications. Like other region-growing methods, the process starts at a point inside the ROI and grows in all directions to extend the region. A boundary voxel is joined to the current region if it has the lowest gray level among the neighbors of the region. This induces a directional growth such that the pixels of low gray level are absorbed first. When several pixels with the same gray level jointly become the candidates for inclusion, a first-come first-served strategy is applied. If the process starts from a local minimum inside the lesion, pixels with monotonically higher and higher gray levels will sequentially join the region. A property of the region, called *peripheral contrast*, is computed for every region during the growing process. This measure corresponds to the difference of the average gray level of the "internal boundary" (the set of outermost connected voxels of the current region) and the "current boundary" (the set of voxels adjacent to the current region). The region with the lowest *peripheral contrast* is selected as the final output.

Since a lesion may have junctions with other low-intensity compartments (e.g., CSF, bone), the region-growing method, as described above, would eventually grow into some neighboring region outside the lesion. To prevent this "spilling over" effect, a criterion based on the size of this neighboring region is employed. Assume the growing region already contains k voxels and the intensity y_k of the last voxel is the highest in the region, $y_{\max} = y_k$. A new candidate y_{k+1} is being considered for inclusion.

- If $y_{k+1} \geq y_{\max}$, the candidate is joined and labeled as belonging to the growing region. The maximum value is updated: $y_{\max} = y_{k+1}$. The growing process then continues by considering the next candidate (the lowest intensity point in its current boundary).
- If $y_{k+1} < y_{\max}$, the candidate is temporarily joined to the growing region and labeled as a possible neighboring subregion. The growing process continues until the intensity of a candidate y_{k+i} is higher than y_{\max} : $y_{k+i} > y_{\max}$. The number of voxels labeled as a possible subregion, i , is then compared with a size threshold, L .
- If $i > L$, a "spilling over" into a low-intensity neighboring region is assumed. Thus, voxels $\{k+1, \dots, k+i\}$ belonging to the subregion are discarded. Then, the growing process continues by considering a new candidate, y_{k+1} (the next lowest gray level in the boundary of the growing region consisting of k voxels).
- If $i < L$, all subregion voxels are permanently joined to the growing region, which now contains $k+i$ voxels. The growing process continues by considering the next candidate (the lowest intensity point in its current boundary).

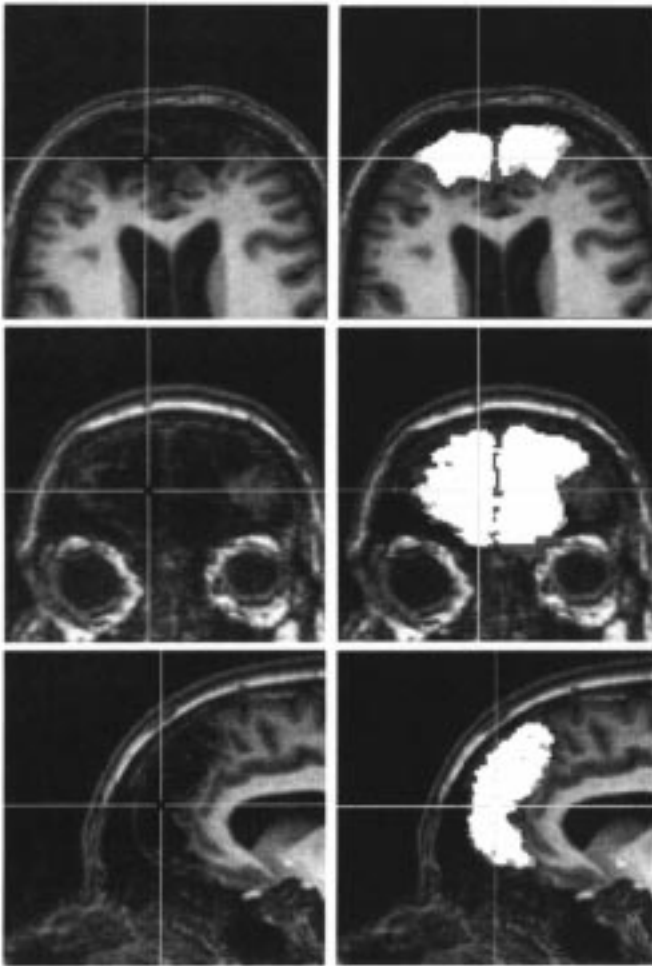


Fig. 1. (left) Sections from a three-dimensional brain data set of case 1 with a bifrontal lesion. (right) Segmentation and annotation of left and right-hemispheric lesions overlaid on the original image.

As a consequence, for small L , the gray level mapping of the sequence of voxels joined to the region shows a smooth change in relation to the voxels inside the lesion.

The behavior of the algorithm is now demonstrated with the left prefrontal lesion of case 1 (Fig. 1). A starting point is chosen inside the left lesion at the crosspoint of the two lines. A size threshold of $L = 3000$ voxels (3.0 cm^3) denotes that the size of the CSF compartment is larger than 3000 voxels and any subregion inside the lesion is expected to be smaller than this value. Fig. 2 shows the intensity of voxels joined during the growing process. To produce a clear figure, only a few cases of over-growing are illustrated. The gray level of considered voxels gradually increases from the starting point, but falls at some stages (e.g., at voxel number 6000, 19000, and 22000, etc). Each of these stages marks a "junction point" which connects the growing region to a neighboring low-intensity subregion. When the size of any subregion exceeds L , it is discarded and the growing process resorts at the junction point and considers to expand the region at the voxel with the next lowest intensity. Thus, the intensity mapping of joined voxels increases more smoothly as opposed to the mapping of considered voxels during the growing process. When the region overgrows into a low-intensity subregion, the *peripheral contrast* increases. Since the size criterion forces the algorithm to absorb only small subregions with low-intensity voxels, the *peripheral contrast* and intensity mappings exhibit a smooth change. The noisy behavior of the *peripheral contrast* at the beginning of the growing process is caused by the highly varying in-

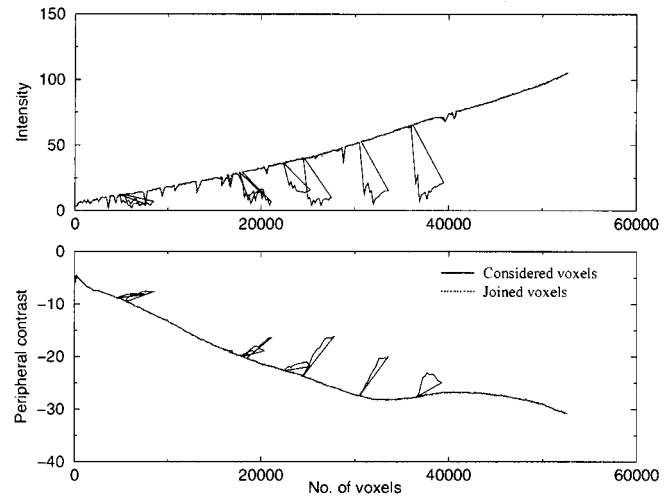


Fig. 2. (top) Gray level mappings and (bottom) *peripheral contrast* during the growing process of the left-hemispheric lesion of case 1.

tensity of voxels joined to the current region when the size of the current region and its current boundary are still small.

In order to determine the best region corresponding to the segmented lesion, the *peripheral contrast* graph is scanned in intervals of L voxels for local minima. From this list, a local minimum is discarded if it is higher than a neighboring minimum. The region corresponding to the first local minimum of the remaining list is accepted as the segmentation result. In the experiment above, the minimum at voxel number 32000 was chosen to specify the segmented lesion.

A postprocessing step is applied to remove some thin structures (junctions between the lesion and the CSF compartment). An opening filter with a spherical structuring element of three-voxel diameter is used here.

III. EXPERIMENTS AND RESULTS

The performance of this algorithm was studied on 8 large lesions from five brain data sets of patients suffering from severe head trauma. MR scans were obtained during their treatment at the Neuropsychological Day-Care Clinic at the University of Leipzig (Leipzig, Germany). A modified driven equilibrium fourier transform (MDEFT) protocol [7] was used to collect high-resolution, T_1 -weighted data sets on a 3.0-T Bruker Medspec 100 system (128 sagittal slices of 256×256 voxels; FOV: 250 mm; slice thickness: 1.4 mm; and subsequent trilinear interpolation to an isotropical resolution of 1 mm).

The starting point required for the segmentation algorithm was chosen manually inside every lesion. A size threshold of $L = 3000$ voxels (3.0 cm^3) was chosen, which is much smaller than the size of CSF compartment, but larger than any subregion inside the lesion.

The segmentation results on five brain datasets were analyzed qualitatively by visual inspection of every slice of the data sets. Examples are shown in Figs. 1, 3, and 4. The algorithm could successfully segment the lesion indicated by the starting point. In one example (Fig. 4), the left- and right-hemispheric lesions were segmented as a single object. Here, both cortical layers were completely damaged, which made an over-growing into the lesion on the contralateral side possible. A separation would be only possible in this case if anatomical knowledge were included.

To validate results, two lesions are manually segmented by a neuroanatomist using our image processing environment [6]. Fig. 1 (right) shows the annotation (in white and light gray) in comparison with the segmentation result (in white and dark gray). Correctly labeled voxels are shown in white [true positive (TP)], the false positive (FP) voxels

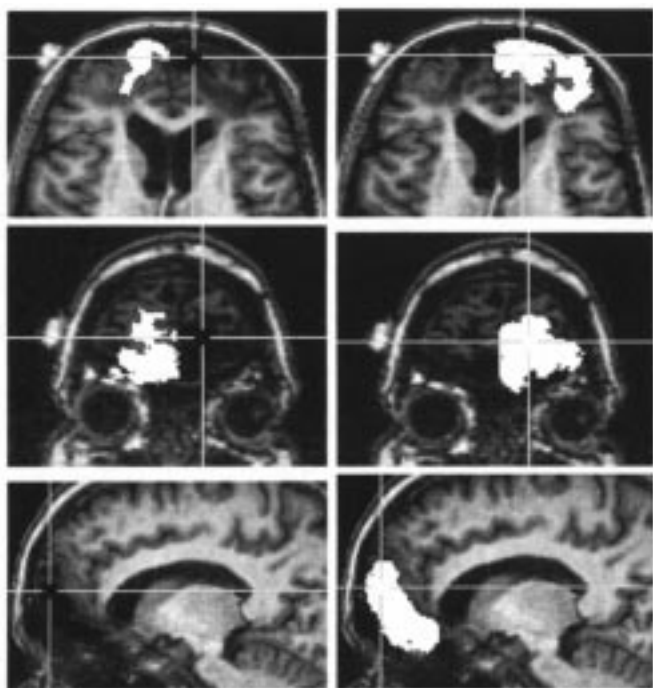


Fig. 3. Segmentation of bifrontal lesions in case 2. Left- and right-hemispheric lesions are segmented separately.

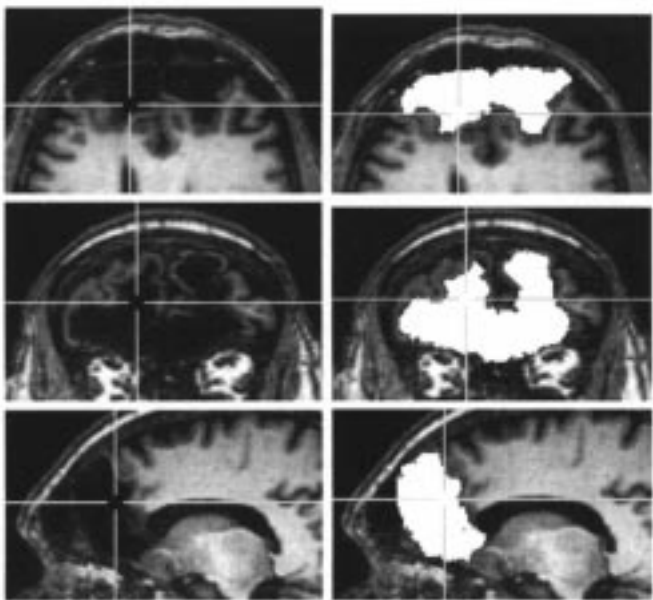


Fig. 4. Segmentation of bifrontal lesions in case 3. Based on intensity, lesions are indistinguishable at basal portions, so only a single lesion is found.

in dark gray and those voxels which are missed by the algorithm are shown in light gray [false negative (FN)]. A quantitative analysis was carried out by comparing the volume of every segmented lesion with that of the annotations. In Table I, TP, FN, and FP rates are compiled as the fraction of voxels in the white, light, and dark gray parts with respect to the total number of voxels in the annotated lesion. FP rates are acceptable given the uncertainty caused by the lack of a well-defined boundary in parts of the lesion and the partial volume effect at boundary voxels. In a lesion of 20 000 voxels (as found in the case examples), increasing the lesion diameter by just one voxel increases its volume by 18%.

TABLE I
TP AND FP RATES (%) FOR VOXELS IN THE SEGMENTED LESION WITH
RESPECT TO THE MANUAL SEGMENTATION

	TP	FP	FN
left lesion	91	15	9
right lesion	88	19	12
both lesions	90	15	10

IV. DISCUSSION

A method was presented to segment large low-intensity lesions from T_1 -weighted MR images of the head. A region-growing technique is governed by a global discontinuity measure to choose the highest gradient region from the set of evolving regions and by a size criterion to prevent from over-growing into other low-intensity compartments of the image.

Since the algorithm locates the lesion boundary based on changes in the gray level mapping of voxels, rather than their absolute values, it is resilient to global differences in image brightness, which are typical in large MR databases. However, results may be affected by local brightness changes due to inhomogeneities of the B_1 field of the scanner. The only parameter of the algorithm, the size threshold L , is used to discriminate homogeneous subregions of a lesion from other low-intensity compartments. Its setting is not critical and does not effect the final result. A manually specified starting point is required to indicate a lesion. While the algorithm is able to segment small lesions (e.g., caused by MS or microangiopathies), lesions in such diseases are typically numerous, and specifying starting points might be considered impractical.

Improvements are possible if anatomical knowledge is included: Starting points might be generated automatically in regions which differ substantially in their intensity distribution from a model [5]. In case 3, an over-growing into the contralateral hemisphere was noticed. Here, both intensity and size criteria fail to produce separate lesions, although the CSF compartment is almost completely excluded. A model-based criterion might be joined in order to prevent from growing into the contralateral hemisphere, i.e., crossing the mid-sagittal plane.

The primary intent of this study was to segment lesions from focal brain damages caused by cerebral infarctions, hemorrhages, or contusions, which are typically low-intensity in T_1 -weighted images. Signal-intense lesions (e.g., certain brain tumours and fresh intracerebral blood) might be segmented as well, if the intensity criterion is reversed. Problems are expected with lesions which feature mixed low- and high-intensity subregions (e.g., highly malignant astrocytomas).

The algorithm as presented here is targeted to work on high-resolution T_1 -weighted images. While multichannel data certainly offer more information to define tissue characteristics [8], [12] and, thus, better criteria to segment a lesion from surrounding tissues, generating high-resolution MR data sets in different weightings is almost prohibitive in terms of acceptable scanning time for a patient.

Results in a series of pathological data sets show a high reliability of the proposed algorithm. Size errors of detected lesions were in the same order as the interrater reliability reported in other studies [1], [11]. The method presented here offers an efficient and reliable alternative to the tedious manual process of lesion segmentation.

REFERENCES

- [1] F. Bello and A. C. F. Colchester, "Measuring global and local spatial correspondence using information theory," in *Lecture Notes in Computer Science*. Heidelberg, Germany: Springer, 1998, vol. 1496, Medical Image Computing and Computer-Assisted Intervention—MICCAI'98, pp. 964–973.

- [2] A. O. Boudraa, S. M. Dehak, Y. M. Zhu, C. Pachai, Y. G. Bao, and J. Grimaud, "Automated segmentation of multiple sclerosis lesions in multispectral MR imaging using fuzzy clustering," *Comput. Biol. Med.*, vol. 30, pp. 23–40, 2000.
- [3] S. A. Hojjatoleslami and J. Kittler, "Region growing: a new approach," *IEEE Trans. Imag. Processing*, vol. 7, pp. 1079–1083, July 1998.
- [4] M. A. Jacobs, R. A. Knight, H. Soltanian-Zadeh, Z. G. Zheng, A. V. Goussev, D. J. Peck, J. P. Windham, and M. Chopp, "Unsupervised segmentation of multiparameter MRI in experimental cerebral ischemia with comparison to T2, diffusion, and ADC MRI parameters and histopathological validation," *J. Magn. Reson. Imaging*, vol. 11, pp. 425–437, 2000.
- [5] M. Kamber, R. Shinghal, L. Collins, G. S. Francis, and A. C. Evans, "Model based 3-D segmentation of multiple sclerosis lesions in magnetic resonance brain images," *IEEE Trans. Med. Imag.*, vol. 14, pp. 442–453, Sept. 1995.
- [6] F. Kruggel and G. Lohmann, "BRIAN (brain image analysis)—a tool for the analysis of multimodal brain data sets," in *Computer Aided Radiology*, R. Inamura, Ed. Amsterdam, The Netherlands: Elsevier, 1996, pp. 323–328.
- [7] J. H. Lee, M. Garwood, R. Menon, G. Adriany, P. Andersen, and K. Ugurbil, "High contrast and fast three-dimensional magnetic resonance imaging at high fields," *Magn. Reson. Med.*, vol. 34, pp. 308–312, 1995.
- [8] K. V. Leemput, F. Maes, F. Bello, D. Vandermeulen, A. C. Colchester, and P. Suetens, "Automated segmentation of ms lesions from multi-channel MR images," in *Lecture Notes in Computer Science*. Heidelberg, Germany: Springer, 1999, vol. 1679, Medical Image Computing and Computer-Assisted Intervention—MICCAI'99, pp. 11–21.
- [9] J. P. Thirion and G. Calmon, "Deformation analysis to detect and quantify active lesions in three-dimensional medical image sequences," *IEEE Trans. Med. Imag.*, vol. 18, pp. 429–441, May 1999.
- [10] R. P. Velthuizen, L. P. Clarke, S. Phuphanich, L. O. Hall, A. M. Bensaid, J. A. Arrington, H. M. Greenberg, and M. L. Silbiger, "Unsupervised measurement of brain tumor volume on MR images," *J. Magn. Reson. Imag.*, vol. 5, pp. 594–605, 1995.
- [11] A. P. Zijdenbos, B. M. Dawant, R. A. Margolin, and A. C. Palmer, "Morphometric analysis of white matter lesions in MR images: method and validation," *IEEE Trans. Med. Imag.*, vol. 13, pp. 716–724, Dec. 1994.
- [12] A. P. Zijdenbos, R. Forghani, and A. C. Evans, "Automatic quantification of ms lesions in 3D MRI brain data sets: validation of insect," in *Lecture Notes in Computer Sciences*. Heidelberg, Germany: Springer, 1998, vol. 1496, Medical Image Computing and Computer-Assisted Intervention—MICCAI'98, pp. 439–448.